

Catalysis Science & Technology

Accepted Manuscript



This is an *Accepted Manuscript*, which has been through the Royal Society of Chemistry peer review process and has been accepted for publication.

Accepted Manuscripts are published online shortly after acceptance, before technical editing, formatting and proof reading. Using this free service, authors can make their results available to the community, in citable form, before we publish the edited article. We will replace this *Accepted Manuscript* with the edited and formatted *Advance Article* as soon as it is available.

You can find more information about *Accepted Manuscripts* in the [Information for Authors](#).

Please note that technical editing may introduce minor changes to the text and/or graphics, which may alter content. The journal's standard [Terms & Conditions](#) and the [Ethical guidelines](#) still apply. In no event shall the Royal Society of Chemistry be held responsible for any errors or omissions in this *Accepted Manuscript* or any consequences arising from the use of any information it contains.

Heterogeneous Double-Activation Catalysis: Rh Complex and Tertiary Amine on Same Solid Surface for the 1,4-Addition Reaction of Aryl- and Alkylboronic Acids

Hiroto Noda, Ken Motokura, Wang-Jae Chun, Akimitsu Miyaji, Sho Yamaguchi, Toshihide Baba*

Department of Environmental Chemistry and Engineering, Tokyo Institute of Technology, 4259 Nagatsuta-cho, Midori-ku, Yokohama, 226-8502, Japan

Graduate School of Arts and Sciences, International Christian University, Mitaka, Tokyo, 181-8585, Japan

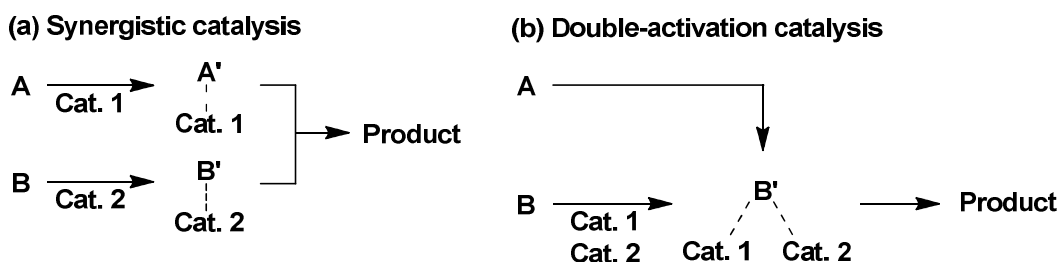
Abstract

Double-activation catalysis by a rhodium complex/tertiary amine catalyst for the 1,4-addition of organoboronic acids was investigated. A rhodium complex and a tertiary amine were co-immobilized on the same silica surface by silane-coupling reactions followed by complexation of the Rh species. Structures of the Rh complex and tertiary amine on the silica surface were determined by solid-state ^{13}C and ^{29}Si MAS NMR, XAFS, and XPS measurements. The immobilized tertiary amine accelerated the Rh-catalyzed 1,4-addition of phenylboronic acid to cyclohexenone. The role of the anchored tertiary amine in the 1,4-addition reaction was clarified by solid-state ^{11}B MAS NMR: it activates the arylboronic acid forming a four coordinate boron species, which then accelerates the transmetallation step in the Rh complex-catalyzed 1,4-addition. The silica-supported Rh complex/tertiary amine catalyst system could be applicable to the reaction of various aryl- and even alkyl-boronic acids.

Keywords: Double-Activation Catalysis, Heterogeneous Catalyst, Silica Support, Tertiary Amine, Rhodium Complex, Organoboronic Acid, 1,4-Addition.

Introduction

Intense research activity has been devoted to the development of concerted catalysis for the acceleration of a single transformation.^[1] Such catalytic systems can be classified as follows: (i) *synergistic catalysis* (Scheme 1a),^[2] and (ii) *double-activation catalysis* (Scheme 1b).^[3] When two substrates (A and B) are activated by two different catalysts simultaneously to accelerate a single transformation, the catalysis system is classified as synergistic (Scheme 1a). In contrast, when two separate catalysts both activate only one of the reactants (B) concertedly, the process is classified as double-activation catalysis (Scheme 1b).

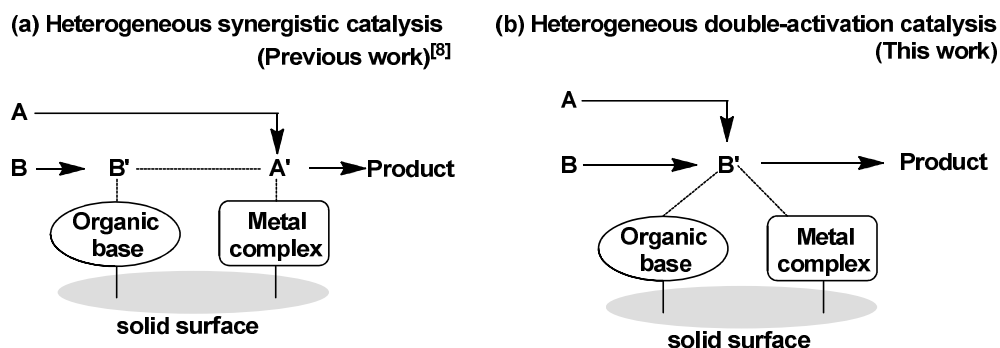


Scheme 1. Classification of catalytic systems involving two catalysts accelerating a single transformation.

To realize reaction systems involving two catalytic sites, the co-immobilization of those sites on the same solid surface is a key strategy. A solid surface enables incompatible catalytic species to co-exist by suppressing their interactions, and allow the close accumulation of catalytic functionalities; therefore, heterogeneous catalysts could have potential utility in the acceleration of a variety of organic transformations by synergistic and double-activation catalysis. For example, heterogeneous multifunctional catalysts having protonic acids, metal nanoparticles, metal cations, and metal complexes

with organic bases on the same surface have been demonstrated.^[4-7]

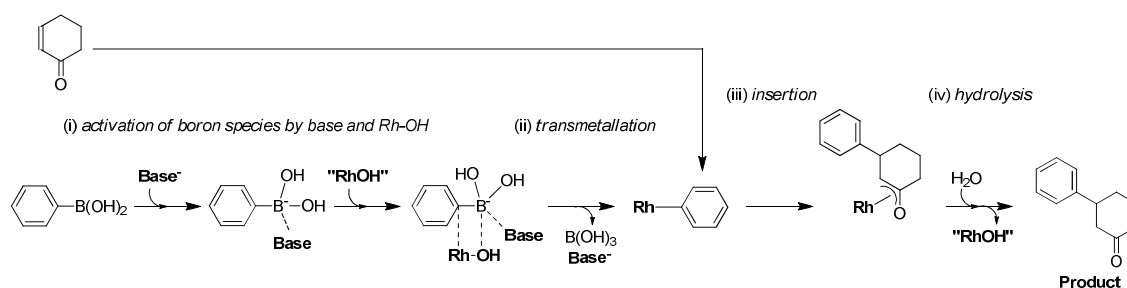
Scheme 2(a) displays heterogeneous synergistic catalysis by a metal complex and organic base on the same solid surface. Our group previously reported heterogeneous synergistic catalysis by a Pd complex and tertiary amine on a silica surface for the Tsuji-Trost allylation.^[8] In the reaction, the Pd complex activates an allylating reagent to form a η^3 -allylpalladium species while the tertiary amine simultaneously activates a nucleophile by abstraction of an α -proton. In this catalysis system, the addition of a homogeneous amine decreased the catalytic activity,^[8] which indicated that self-quenching was avoided by anchoring both the metal complex and the amine. When catalytic sites are immobilized on the same surface, they can co-exist and activate substrates simultaneously.



Scheme 2. Metal complex and organic base on same surface for heterogeneous (a) synergistic and (b) double-activation catalysis.

On the basis of the previous results, we hypothesized that a surface co-immobilization strategy could extend to double-activation catalysis (Scheme 2b). One reaction potentially amenable to *heterogeneous double-activation catalysis* is the 1,4-addition of an arylboronic acid to an α,β -unsaturated carbonyl compound catalyzed by a Rh

complex.^[9] The 1,4-addition of arylboron reagents to enones is a widely used reaction for C–C bond formation, giving β -substituted carbonyl compounds.^[9] It is known that the reaction is accelerated by bases.^[9c,j] Scheme 3 shows the reaction mechanism for 1,4-addition in the presence of a base. The catalytic cycle using a Rh–OH complex with a base involves (i) activation of the arylboronic acid by the base to form a 4-coordinate boron species; (ii) transmetalation of the aryl group from the activated boron to Rh; (iii) insertion of the α,β -unsaturated carbonyl compound into the aryl–Rh bond; and (iv) hydrolysis, giving the 1,4-addition product and the Rh–OH species. Transmetalation step (ii), which is usually rate-limiting,^[10] proceeds smoothly when an arylboronic acid is activated by base to form the 4-coordinate boron species.^[11] This activation mechanism is one of *double-activation catalysis* because $\text{PhB}(\text{OH})_2$ can be activated by both the base and the Rh species. Actually, Hara and co-workers very recently reported the highly efficient 1,4-addition reaction of arylboronic acids catalyzed by a Rh complex with a OH^- site in a layered material.^[9m]



Scheme 3. Mechanism of 1,4-addition of phenylboronic acid to cyclohexenone catalyzed by a Rh–OH complex and base.

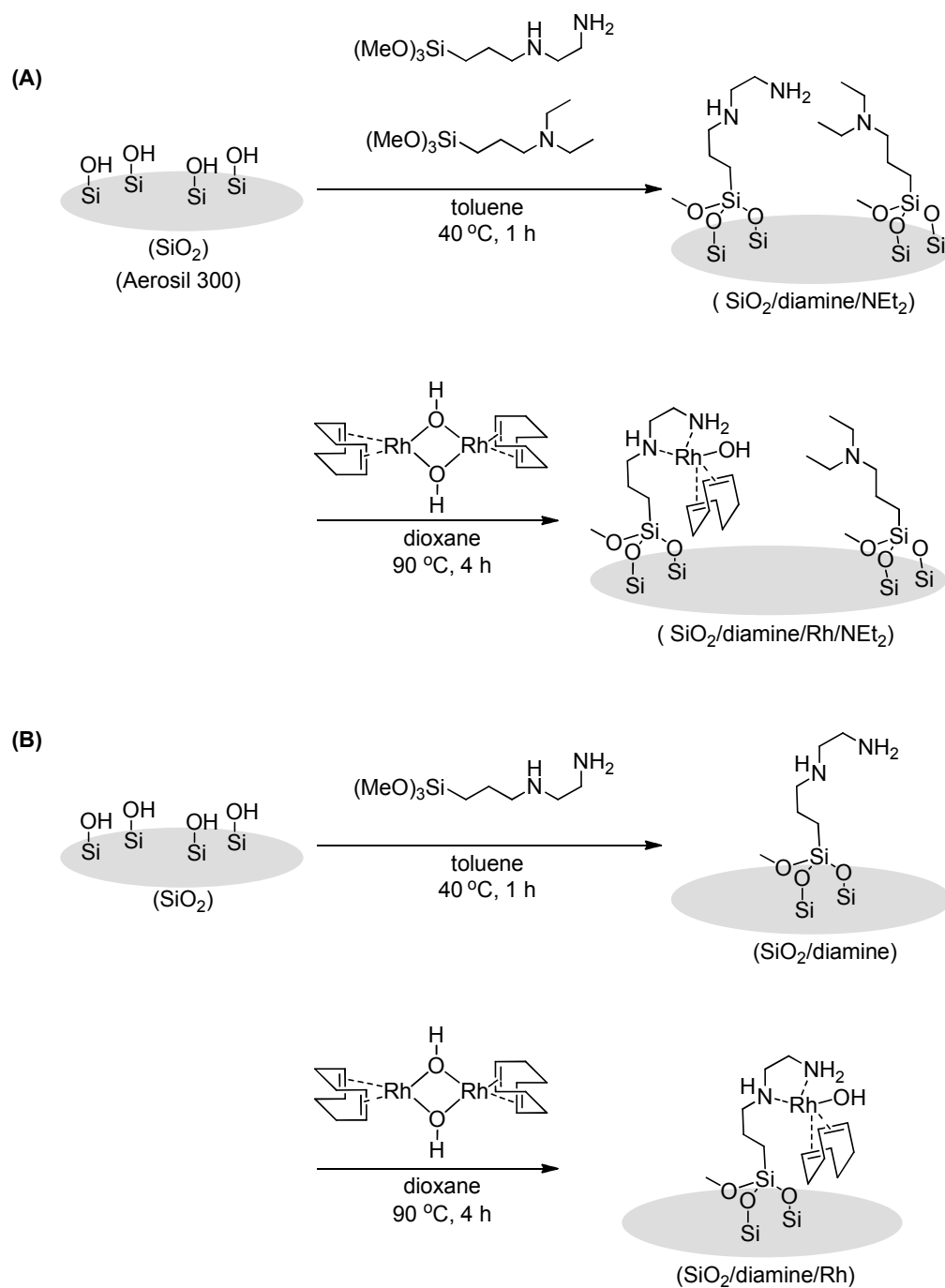
Here, we predicted that, if a Rh complex and an organic amine existed closely on the same solid surface, the amine would trap the arylboronic acid as the 4-coordinate boron species,^[12] ensuring proximity of the activated boron species to the Rh complex, and thus accelerate the transmetalation step. In addition, we speculated that a strong Lewis base, which would be incompatible with the active Rh complex in a homogeneous system, could co-exist with that complex in a heterogeneous system and should powerfully activate poor reactive substrate such as alkylboronic acid.

Herein, we demonstrate heterogeneous double-activation catalysis by a Rh complex and tertiary amine on a silica surface. The silica-supported tertiary amine accelerates the Rh complex-catalyzed 1,4-addition of arylboronic acids to α,β -unsaturated carbonyl compounds. We also clarify the mechanism of the anchored tertiary amine-accelerated reaction catalyzed by a Rh complex on the same surface. The catalyst system could be applicable for the 1,4-addition reaction using various aryl- and alkyl-boronic acids.

Results and discussion

Catalyst preparation and characterization

Scheme 4A shows a typical procedure for the synthesis of the silica-supported rhodium complex/tertiary amine catalyst ($\text{SiO}_2/\text{diamine}/\text{Rh}/\text{NEt}_2$). 3-(2-Aminoethylamino)-propyltrimethoxysilane and 3-diethylaminopropyltrimethoxysilane were immobilized on SiO_2 using a silane-coupling reaction to afford the silica-supported amines ($\text{SiO}_2/\text{diamine}/\text{NEt}_2$). This material was treated with $[\text{Rh}(\text{cod})\text{OH}]_2$ (equimolar with the immobilized diamine) in dioxane solvent to afford $\text{SiO}_2/\text{diamine}/\text{Rh}/\text{NEt}_2$. A catalyst having only the rhodium complex immobilized on silica ($\text{SiO}_2/\text{diamine}/\text{Rh}$, Scheme 4B) was also prepared using the silane-coupling reaction followed by complexation.



Scheme 4. Syntheses of (A) SiO₂/diamine/Rh/NET₂ and (B) SiO₂/diamine/Rh catalysts.

Table 1 summarizes the elemental analysis results of the prepared samples. The presence of carbon and nitrogen in all samples indicates the incorporation of the organic amines. For example, SiO₂/diamine/Rh-a contained a 6.38 mmol/g of carbon, 1.07 mmol/g of nitrogen, and 0.528 mmol/g of rhodium atom. The C/N/Rh ratio was 12/2/1, which is consistent with the theoretical ratio (Scheme 4B). When the charged amount of the silane-coupling reagent was decreased, a catalyst having reduced organic and Rh contents was obtained (SiO₂/diamine/Rh-b). This indicates that the amount of immobilized complex is easily controlled by changing the raw material loading. The SiO₂/diamine/Rh/NEt₂-a catalyst had an 8.21 mmol/g of carbon, 1.31 mmol/g of nitrogen, and 0.412 mmol/g of rhodium atom. The Rh/N ratio was 1/3, which suggests the presence of almost equimolar amounts of the diamine-rhodium complex and tertiary amine. As will be described in the spectroscopic analysis discussion, all the diamines on the SiO₂ surface coordinated to Rh centers after the complexation reaction. Therefore, the amount of tertiary amine on the SiO₂/diamine/Rh/NEt₂-a catalyst was calculated to be 0.44 mmol/g based on the amount of Rh and total N content. The amounts of N and Rh in the prepared samples were found to correspond closely to the amounts of the introduced raw materials, silane-coupling reagents, and Rh precursor. This enables the preparation of catalysts that differ in the total amounts and ratios of organic functionalities (Rh complex and tertiary amine group) by selecting the corresponding raw material charges. Catalysts which contained (i) approximately 0.06 mmol/g Rh complex and various quantities of tertiary amine (SiO₂/diamine/Rh/NEt₂-b, c, and d), and (ii) various amounts of organic functionalities with similar ratios of tertiary amine/Rh (ca. 1/1) (SiO₂/diamine/Rh/NEt₂-a, e-g) were also prepared. For these catalysts, the elemental analysis results were in agreement with the theoretical values.

The immobilization of organic functionalities on the silica surface was confirmed by solid-state ^{29}Si magic angle spinning (MAS) NMR spectroscopy (Figure S1). The ^{29}Si NMR spectrum of $\text{SiO}_2/\text{diamine}/\text{Rh}/\text{NEt}_2\text{-a}$ presented two groups of typical signals (Figure S1B; Q and T sites) distributed from -90 to -130 ppm and from -50 to -70 ppm, respectively. In the spectrum, the upfield Q signals originate from silica, whereas the downfield T sites are derived from the immobilized silane-coupling reagents. The T site [$\text{T}^m = \text{R}\text{Si}(\text{OH})_{3-m}(\text{OSi})_m$] was observed to appear after immobilization (cf. Figures S1A and S1B). In the parent SiO_2 , the Q sites showed three signals at -111 , -101 , and -91 ppm, corresponding to the Q^4 , Q^3 , and Q^2 species of the silica framework, respectively [$\text{Q}^n = \text{Si}(\text{OSi})_n(\text{OH})_{4-n}$]. After the silane-coupling reaction, the $\text{Q}^3/(\text{Q}^2 + \text{Q}^3 + \text{Q}^4)$ ratio decreased from 0.23 to 0.17 and the $\text{Q}^2/(\text{Q}^2 + \text{Q}^3 + \text{Q}^4)$ ratio decreased from 0.02 to <0.01 . The decrease in silanol content was calculated to be 1.5 mmol/g.^[13] This value is reasonable in comparison with the elemental analysis results for the $\text{SiO}_2/\text{diamine}/\text{Rh}/\text{NEt}_2\text{-a}$ (Table 1). These ^{29}Si MAS NMR data indicate that the organic reagents are immobilized on the silica surface by Si(surface)–O–Si covalent bonding.^[14]

To clarify the structures of the Rh complexes and tertiary amines anchored on the silica surface, ^{13}C cross polarization (CP)/MAS NMR measurements were acquired (Figure 1). No significant shifts were observed in the spectra before and after immobilization of the diamine and tertiary amine functionalities (cf. Figure 1A and 1B with Figure 1C), except for the carbons adjacent to silicon atoms. These results indicate that the organic amines are anchored on the SiO_2 surface while maintaining their carbon skeletons. Figure 1D displays the ^{13}C NMR spectrum of $\text{SiO}_2/\text{diamine}/\text{Rh}\text{-a}$. After treatment of the $\text{SiO}_2/\text{diamine}$ with $[\text{Rh}(\text{cod})\text{OH}]_2$, the signal derived from the carbon next to the nitrogen atom was shifted to lower field [$42 \rightarrow 43$ ppm (\blacktriangle)], and that of the central

carbon in the propyl chain was shifted to higher field [24 → 22 ppm (●)]. The signal derived from the olefinic carbons of the cyclooctadiene ligand (cod) was also shifted from 73 to 80–90 ppm.^[15] These changes in the ¹³C NMR chemical shifts indicate complexation of the Rh species with the ethylenediamine function on the silica surface. Figure 1E shows the ¹³C NMR spectrum of SiO₂/diamine/Rh/NEt₂-a. Comparing the spectra before and after complexation (Figure 1E versus 1C), similar shifts for the SiO₂/diamine/Rh-a component (Figure 1D) were observed, which indicates that the complexation of ethylenediamine also occurs in case of SiO₂/diamine/NEt₂-a. Moreover, signals derived from the tertiary amine did not shift after complexation, (cf. the peak at 56 ppm (◇)), suggesting that tertiary amine moiety does not have any interaction with the Rh complex on the silica surface.

To clarify the acceleration effect of the immobilized tertiary amine on the Rh-catalyzed reaction, it was necessary to confirm that the prepared catalysts possessed the same local structure for the Rh complex in both the presence and absence of the surface-bound tertiary amine. To determine the local structure and electronic state of the immobilized Rh complex, X-ray absorption fine structure (XAFS) measurements were conducted. Figure 2 shows the Rh K-edge X-ray absorption near-edge structure (XANES) spectra of the prepared silica-supported Rh catalysts together with those of Rh⁰ foil, Rh^{III}₂O₃, and [Rh^I(cod)OH]₂ as reference samples. The absorption edge varies with respect to the oxidation state of the rhodium. The XANES spectrum of the Rh foil has two distinct peaks around 23,230 and 23,256 eV (Figure 2A). In case of Rh₂O₃, the spectrum has two peaks around 23,232 and 23,244 eV (Figure 2B). On the other hand, the spectrum of the [Rh(cod)OH]₂ has one broad peak around 23,236 eV (Figure 2C). The spectral features of the silica-supported catalyst (SiO₂/diamine/Rh/NEt₂-a, Figure

2D) resemble that of the monovalent complex, which indicates that the Rh species in the catalyst is in the +1 oxidation state. X-Ray photoelectron spectroscopy (XPS) analysis of Rh $3d_{5/2}$ also indicates that the surface Rh species is Rh(I) (Binding energy = 308.5–308.9 eV) (Figure S2).^[16] These XANES and XPS results strongly indicate that the absence of metallic Rh particle on the SiO₂ surface. In the case of SiO₂/diamine/Rh-a without the tertiary amine groups (Figure 2E), the XANES spectrum was almost identical to that of SiO₂/diamine/Rh/NEt₂-a, which also indicates the monovalent state of the Rh species. In comparing the catalysts SiO₂/diamine/Rh/NEt₂-b and -f with SiO₂/diamine/Rh/NEt₂-a, similar spectra are observed (Figure S3), which indicates that the loading of the Rh complex on the SiO₂ surface (0.054–0.412 mmol g⁻¹) does not affect its oxidation state. After the catalytic 1,4-addition reaction, the recovered SiO₂/diamine/Rh/NEt₂-a maintained the +1 oxidation state (Figure 2F).

The k^3 -weighted extended X-ray absorption fine structure (EXAFS) spectrum of SiO₂/diamine/Rh/NEt₂-a is almost identical to those of SiO₂/diamine/Rh-a and SiO₂/diamine/Rh/NEt₂-b (Figure 3). Thus, the local structure of the Rh complex is not affected by the presence of the tertiary amine and the loading amounts of the organic functionalities. Moreover, the recovered SiO₂/diamine/Rh/NEt₂-a was also consistent with the fresh catalyst (Figure S4), which indicates that the local structure of the Rh complex used for the reaction is maintained.

Figure 4 shows the Fourier transforms (FT) of the k^3 -weighted EXAFS spectra of the prepared catalysts and the reference samples (Rh⁰ foil, Rh^{III}₂O₃, and [Rh^I(cod)OH]₂). Rh foil has a strong peak around 2.4 Å, derived from Rh–Rh bonds (Figure 4A). The peaks around 1.6 and 2.5 Å in the Rh₂O₃ spectrum can be identified as Rh–O and Rh–O–Rh bonds, respectively (Figure 4B). [Rh(cod)OH]₂ has two peaks

around 1.7 and 2.6 Å, derived from Rh–C/O and Rh–O–Rh, respectively (Figure 4C). In the spectrum of the SiO₂/diamine/Rh/NEt₂-a, two peaks can be observed around 1.6 and 2.5 Å (Figure 4D). The first shell was well fitted by the using Rh–C/O parameter (Figure S5). Table 2 summarizes the results of the curve-fitting analysis of the EXAFS data. In the case of SiO₂/diamine/Rh/NEt₂-a, the coordination number (*N*) in the first shell was evaluated as 6.8. Since EXAFS is not able to distinguish between light-scattering atoms (in this study O, C, N),^[17] this *N* value is consistent with the theoretical value containing four Rh–C bonds, two Rh–N bonds, and one Rh–O bond.^[18] In addition, the peak around 2.5 Å was not fitted with Rh–O–Rh at all, suggesting that the Rh complex in the SiO₂/diamine/Rh/NEt₂-a catalyst did not form a dimeric complex. Overall, the proposed surface structure of SiO₂/diamine/Rh/NEt₂ is shown in Figure 1E. The results of the curve-fitting analyses of the other prepared catalysts are similar to those of SiO₂/diamine/Rh/NEt₂-a and also agree with the theoretical values (Table 2). These curve-fitting results indicate that the local structure of the Rh complex is not affected by its loading and the presence of tertiary amine groups on the same SiO₂ surface.

To summarize, the NMR, XAFS, and XPS analyses show that the (i) Rh species on the prepared catalyst is monovalent; (ii) the local structure of the Rh complex is not affected by the presence of the tertiary amine and the amount of immobilized organic functionalities; (iii) the ligands for the Rh complex on the prepared catalyst include the diamine, cyclooctadiene, and hydroxyl ligands; and (iv) the structure of the Rh complex is maintained after the catalytic 1,4-addition reaction.

1,4-Addition reaction using silica-supported Rh catalyst

The 1,4-addition reaction between cyclohexenone (**1**) and phenylboronic acid (**2**) in the presence of the Rh catalysts was examined; the results are summarized in Table 3. Product **3** was obtained in 28% yield when using SiO₂/diamine/Rh/NEt₂-a, which contains both the immobilized Rh complex and the tertiary amine (Table 3, entry 1). The yield was 10% for SiO₂/diamine/Rh-a (Table 3, entry 2). Without the rhodium species, the reaction did not proceed at all (Table 3, entries 3 and 4), indicating that the Rh complex was necessary to promote the reaction. These results also show that the tertiary amine accelerates the Rh-catalyzed 1,4-addition reaction. When the SiO₂/diamine/Rh-a catalyst was used for the reaction with a homogeneous tertiary amine, the product yield was lower than that in the case of SiO₂/diamine/Rh-a alone (Table 3, entry 5 versus 2). In addition, an increase in the amount of additional free tertiary amine caused a decrease in the catalytic activity (Figure S6). Furthermore, in the case of the SiO₂/diamine/Rh/NEt₂-a catalyst, the presence of free tertiary amine also deactivated the catalyst (Table 3, entry 6 versus 1). The results for entries 5 and 6 indicate that a tertiary amine which is not anchored on the surface inhibits the Rh-catalyzed reaction. The product yield was not enhanced by the addition of SiO₂/NEt₂, i.e., silica with only a tertiary amine, to the reaction mixture with SiO₂/diamine/Rh-a (Table 3, entry 7). To remove the possibility that the enhancement of catalytic activity derived from the decreased amount of surface silanol groups, a catalyst in which the surface silanols had been capped with methyltrimethoxysilane (SiO₂/diamine/Rh/Me) was tested. The catalytic activity was not enhanced compared with SiO₂/diamine/Rh-a (Table 3, entry 8 versus 2).

Next, to confirm that the reaction proceeds on the catalyst surface, a filtration test was

conducted in which the SiO₂/diamine/Rh/NEt₂ catalyst was removed from the reaction mixture by filtration at approximately 35% conversion. After the solid catalyst was removed, the reaction did not proceed further in the filtrate (Figure S7), which indicates that the Rh-catalyzed reaction proceeds at the solid surface. The immobilized tertiary amine enhances the Rh complex-catalyzed reaction on the silica surface.

To investigate the effect of the amount of immobilized tertiary amine on the catalytic activity, catalysts which had similar loadings of the Rh complex and varying amounts of tertiary amine (0.07–0.91 mmol/g) were used for the reaction. The results are summarized in Table 4. Upon increasing the amount of immobilized tertiary amine on the surface, the 1,4-addition product yield increased. This result strongly supports the acceleration of the Rh-catalyzed reaction by the immobilized tertiary amine.

Next, catalysts which had various total amounts of organic functionalities (tertiary amine + Rh complex) with similar Rh complex/tertiary amine ratios (ca. 1/1) were used for the reaction. As shown in Table 5, increasing the total amount of immobilized organic functionalities increased the product yield, suggesting that the catalytic activity depends on the surface density of the organic functionalities.

The SiO₂/diamine/Rh/NEt₂-a and SiO₂/diamine/Rh/NEt₂-d catalysts have nearly equivalent amounts of total organic functionalities, but the loadings of the Rh complex are quite different. However, both catalysts afforded similar product yields (Table 6). In addition, in the cases of SiO₂/diamine/Rh/NEt₂-c and SiO₂/diamine/Rh/NEt₂-f, which both had ca. 0.5 mmol/g total organic functionalities, the same phenomena occurred (Table 6).

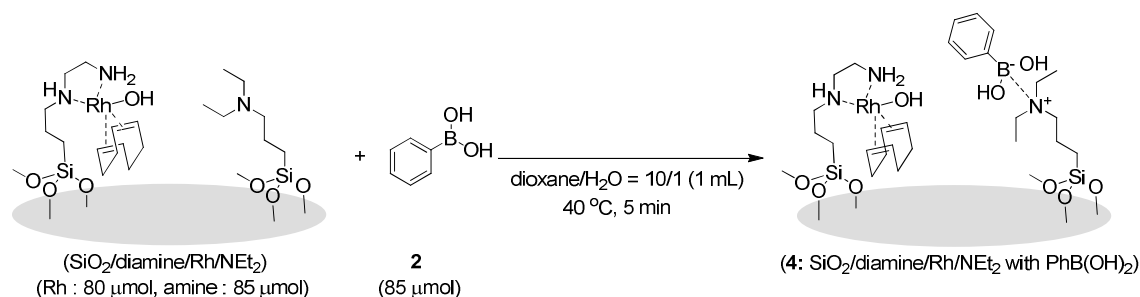
To summarize these catalytic reaction results, we found that (i) the surface tertiary amine accelerates the Rh-catalyzed reaction and (ii) a higher density of the total organic

functionalities leads to high catalytic activity. If the organic functionalities are homogeneously dispersed on the SiO₂ surface, the catalytic activity should depend on the distance between the tertiary amine and Rh complex. Thus, it is strongly suggested that *heterogeneous double-activation catalysis* (Scheme 2b) is effected by the tertiary amine/Rh complex on the SiO₂ surface for the 1,4-addition reaction.

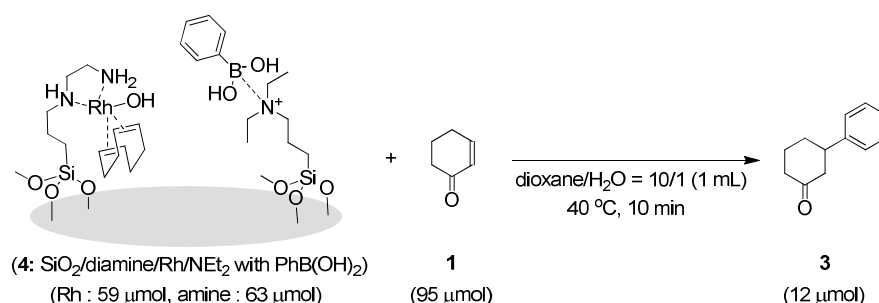
Reaction mechanism

One possible explanation for the acceleration of the 1,4-addition reaction by the tertiary amine is the enhancement of the rate-determining step in the reaction using SiO₂/diamine/Rh catalyst. Kinetic studies show a zero-order dependence on the concentration of cyclohexenone (Figure S8), which indicates that the insertion step (Scheme 3(ii)) proceeds smoothly and is not rate-determining. On the other hand, the first-order dependence on the concentration of phenylboronic acid (Figure S9) shows that the transmetalation step (Scheme 3 (i)) is rate-determining. It is conceivable that the tertiary amine anchored on the silica surface accelerates transmetalation by the formation of 4-coordinate boron species in the catalytic cycle of the reaction. To confirm the formation of such species by reaction of the phenylboronic acid with the immobilized tertiary amine, solid-state ¹¹B MAS NMR measurements were conducted. After the adsorption of PhB(OH)₂ on a silica-supported tertiary amine (SiO₂/NEt₂), a new peak can be observed at around 1.1 ppm (Figure 5). This peak is identified as the four-coordinate boron species,^[19] whereas, three-coordinate sites derived from phenylboronic acid itself cover a larger chemical shift range. The peak at around 1.1 ppm did not appear when SiO₂ was treated with phenylboronic acid. This result indicates that the tertiary amine on the SiO₂ surface coordinates to phenylboronic acid

to afford the 4-coordinate boron species. The formation of this species was also confirmed by ^{11}B multiple-quantum (MQ) MAS NMR measurements (Figure 6). The resonances corresponding to phenylboronic acid were visible in the region from $\delta_{\text{F2}} = -6$ –28 ppm and $\delta_{\text{F1}} = 14$ ppm (B(III)_a; Figure 6A). After the treatment of $\text{SiO}_2/\text{NEt}_2$ with PhB(OH)_2 , the resonances shifted to around $\delta_{\text{F2}} = 0$ and $\delta_{\text{F1}} = 29$ ppm, which were assigned to the four-coordinate boron species (B(IV)_a; Figure 6B). When the $\text{SiO}_2/\text{diamine}/\text{Rh}/\text{NEt}_2\text{-a}$ catalyst was treated with phenylboronic acid (Scheme 5), two signals appeared: B(IV)_a ($\delta_{\text{F2}}:\delta_{\text{F1}} = 0:29$ ppm) and B(IV)_b ($\delta_{\text{F2}}:\delta_{\text{F1}} = 0:25$ ppm) (Figure 6C). The former signal (B(IV)_a) was identified as the four-coordinate phenylboronic acid, and the latter signal (B(IV)_b) was derived from the four-coordinate boronic acid.^[20] This result indicates that the tertiary amine on the $\text{SiO}_2/\text{diamine}/\text{Rh}/\text{NEt}_2\text{-a}$ reacts with phenylboronic acid to form a four-coordinate boron species on the catalyst surface (**4**), as shown in Scheme 5. Next, compound **4** was treated with cyclohexenone (**1**) (Scheme 6). The 1,4-addition reaction proceeded smoothly and product **3** was obtained (Scheme 6). Then, the resonance due to the four-coordinate phenylboronic acid (B(IV)_a) disappeared (Figure 6D). Taken together, these results indicate that the 1,4-addition reaction pathway mediated by $\text{SiO}_2/\text{diamine}/\text{Rh}/\text{NEt}_2$ includes the transmetalation of the tertiary amine-activated four-coordinate boron species on the SiO_2 surface. The transmetalation, which is the rate-determining step of the reaction, is accelerated by the surface tertiary amine, leading to the enhancement of the catalytic activity.

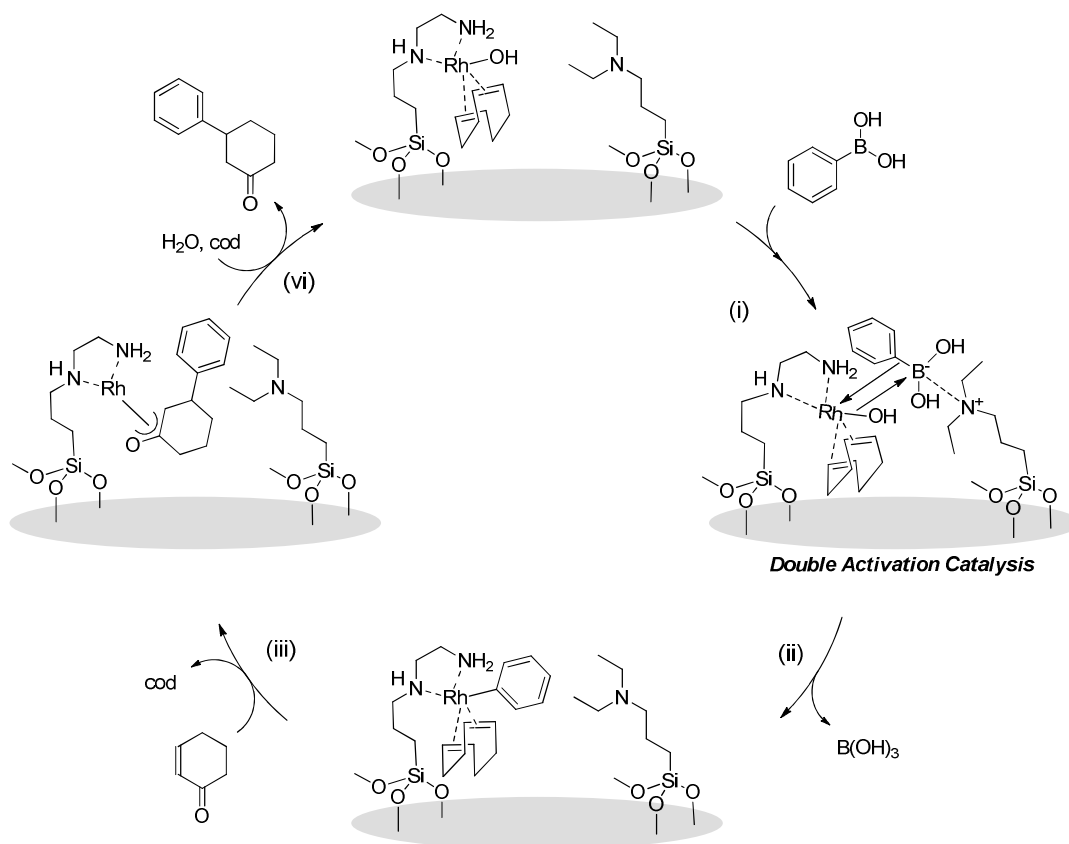


Scheme 5. Treatment of SiO₂/diamine/Rh/NEt₂-a with phenylboronic acid.



Scheme 6. Treatment of **4** with cyclohexenone.

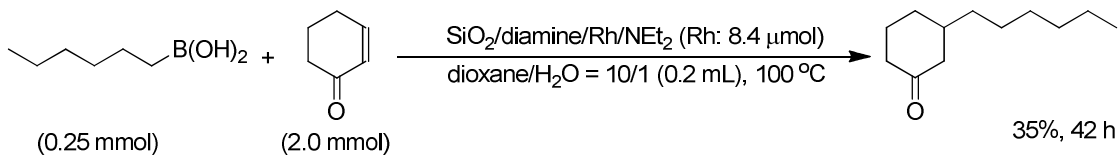
Overall, the proposed mechanism for the transformation in the presence of the SiO₂/diamine/Rh/NEt₂ catalyst is shown in Scheme 7. The catalytic cycle involves (i) formation of the four-coordinate boron species from reaction of the phenylboronic acid with the tertiary amine, (ii) transmetalation of the aryl group from the activated boron species to the Rh complex, (iii) insertion of an α,β -unsaturated carbonyl compound into the aryl–Rh bond, and (iv) hydrolysis, giving the 1,4-addition product and the Rh–OH species.



Scheme 7. Proposed double-activation mechanism of the 1,4-addition reaction in the presence of the $\text{SiO}_2/\text{diamine}/\text{Rh}/\text{NEt}_2$ catalyst.

Substrate Scope and Application

To explore the scope of the SiO₂/diamine/Rh/NEt₂-a catalyzed 1,4-addition reaction, we examined the reaction of various phenylboronic acids with cyclohexenone (**1**). The results are summarized in Table 7. The product yield reached >99% within 1 h in the presence of 12.0 μmol of the rhodium species (Table 7, entry 1). Electron-donating substituents such as methoxy and methyl groups, at the *para* position of the phenyl ring resulted in excellent yields (Table 7, entries 2 and 3). In case of electron-withdrawing groups such as acetyl and chloro moieties, the reaction also proceeded in 80–84% yields (Table 7, entries 4 and 5). The catalyst was also applicable for the reaction using *trans*-2-phenylvinylboronic acid (Table 7, entry 6). The product yield was higher than that in the case of SiO₂/diamine/Rh-a. When a boron ester was used instead of the phenylboronic acid, the SiO₂/diamine/Rh/NEt₂-a catalyst also afforded a higher yield than SiO₂/diamine/Rh-a (Table 7, entry 7). As shown in Scheme 8, the 1,4-addition reaction using an alkylboronic acid as a reactant proceeded in the presence of the SiO₂/diamine/Rh/NEt₂-a catalyst. To the best of our knowledge, this is the first example of 1,4-addition using an alkylboronic acid.



Scheme 8. 1,4-Addition reaction using alkylboronic acid as a reactant.

Conclusions

A silica-supported Rh complex/tertiary amine catalyst was synthesized and characterized. Double-activation catalysis was observed when the surface contained both the immobilized Rh complex and tertiary amine. The presence of the tertiary amine immobilized on the same surface with the Rh complex accelerated the rhodium-catalyzed 1,4-addition of phenylboronic acids to cyclohexenone. The solid-state ^{11}B MQ MAS NMR measurements revealed that the 1,4-addition reaction proceeded through the formation of a four-coordinate boron species from the reaction of the phenylboronic acid with the surface-bound tertiary amine. The catalyst was applied in the reaction of various organoboronic acids, including both aryl and alkyl types.

Acknowledgement

We thank the Kyusyu Synchrotron Light Research Center (SAGA-LS) for their technical support. XAFS measurements were carried out under the approval of the SAGA-LS Advisory Committee (Proposal No. 1404015F). This study was supported by JSPS KAKENHI (grant Nos. 24686092 and 25630362) and JSPS Grant-in-Aid for Scientific Research on Innovative Areas "3D Active-Site Science" (grant No. 26105003). H.N. thanks Grant-in-Aid for JSPS Fellows (grant No. 26•12038).

Experimental Section

Preparation of SiO₂/diamine/NEt₂ and SiO₂/diamine/Rh/NEt₂

SiO₂ (Aerosil[®] 300, 300 m²g⁻¹, SiO₂ content: >99.9%, NIPPON AEROSIL Co.) was pretreated at 120 °C for 3 h under vacuum. Dried SiO₂ (0.64 g) was placed in a round-bottom flask and treated with 15.0 mL of toluene solution containing 3-(2-Aminoethylamino)propyltrimethoxysilane (0.40 mmol, 9.0 × 10⁻² g) and 3-diethylaminopropyltrimethoxysilane (0.40 mmol, 9.5 × 10⁻² g) at 40 °C for 1 h. Toluene was removed by vacuum evaporation, affording SiO₂/diamine/NEt₂. Then, 0.21 g of SiO₂/diamine/NEt₂ was treated with 3.0 mL of dioxane containing [Rh(cod)OH]₂ (5.0 × 10⁻² mmol; Rh: 0.10 mmol) at 90°C for 4 h. The resulting mixture was evaporated and dried under vacuum, affording SiO₂/diamine/Rh/NEt₂-a.

1,4-Addition reaction using silica-supported Rh catalyst

A silica-supported Rh catalyst (6.0 μmol), dioxane/H₂O (10/1, 2.0 mL), cyclohexenone (**1**) (1.0 mmol), and phenylboronic acid (**2**) (1.5 mmol), were placed in a Pyrex glass reactor. The resulting mixture was stirred vigorously for 1 h at 60°C under Ar. Product formation was confirmed by GC-MS and NMR. Yields and conversion were determined by ¹H NMR using a CDCl₃ solution of the reaction mixture.

Treatment of SiO₂/NEt₂ with phenylboronic acid for ¹¹B NMR analysis of the reaction intermediate

SiO₂/NEt₂ (0.10 g, N: 0.083 mmol), dioxane/H₂O (10/1, 1.0 mL), and phenylboronic acid (**2**) (0.083 mmol) were placed in a Pyrex glass reactor. The resulting mixture was

vigorously stirred for 5 min at 40 °C under Ar. Then, the solvent was evaporated under vacuum, and the resulting solid was transferred to the NMR sample rotor.

Treatment of SiO₂/diamine/Rh/NEt₂ with phenylboronic acid for ¹¹B NMR analysis of the reaction intermediate

SiO₂/diamine/Rh/NEt₂ (0.19 g, tertiary amine: 0.085 mmol), dioxane/H₂O (10/1, 1.0 mL), and phenylboronic acid (**2**) (0.085 mmol) were placed in a Pyrex glass reactor. The resulting mixture was vigorously stirred for 5 min at 40 °C under Ar. Then, the solvent was evaporated under vacuum, and the resulting solid was transferred to the NMR sample rotor.

References

- [1] Allen, A. E.; MacMillan, D. W. C. *Chem. Sci.* **2012**, *3*, 633.
- [2] (a) Sawamura, M.; Sudoh, M.; Ito, Y. *J. Am. Chem. Soc.* **1996**, *118*, 3309. (b) Kanemasa, S.; Ito, K. *Eur. J. Org. Chem.* **2004**, 4741. (c) Ibrahim, I.; Córdova, A. *Angew. Chem. Int. Ed.* **2006**, *45*, 1952. (d) Trost, B. M.; Luan, X. *J. Am. Chem. Soc.* **2011**, *133*, 1706.
- [3] (a) Rubina, M.; Conley, M.; Gevorgyan, V. *J. Am. Chem. Soc.* **2006**, *128*, 5818. (b) Mukherjee, S.; List, B. *J. Am. Chem. Soc.* **2007**, *129*, 11336. (c) Xu, H.; Zuend, S. J.; Woll, M. G.; Tao, Y.; Jacobsen, E. N. *Science* **2010**, *327*, 986. (d) Ema, T.; Miyazaki, Y.; Koyama, S.; Yano, Y.; Sakai, T. *Chem. Commun.* **2012**, *48*, 4489.
- [4] For Reviews, see: (a) Margelefsky, E. L.; Zeidan, R. K.; Davis, M. E. *Chem. Soc. Rev.* **2008**, *37*, 1118. (b) Motokura, K.; Tada, M.; Iwasawa, Y. *Chem. Asia J.* **2008**, *3*, 1230.
- [5] For Brønsted acids and organic bases, see: (a) Kubota, Y.; Goto, K.; Miyata, S.; Goto, Y.; Fukushima, Y.; Sugi, Y. *Chem. Lett.* **2003**, *32*, 234. (b) Huh, S.; Chen, H.-T.; Wiench, J. W.; Pruski, M.; Lin, V. S.-Y. *Angew. Chem. Int. Ed.* **2005**, *44*, 1826. (c) Zeidan, R. K.; Hwang, S.-J.; Davis, M. E. *Angew. Chem. Int. Ed.* **2006**, *45*, 6332. (d) Bass, J. D.; Solovyov, A.; Pascall, A. J.; Katz, A. *J. Am. Chem. Soc.* **2006**, *128*, 3737. (e) Motokura, K.; Tada, M.; Iwasawa, Y. *J. Am. Chem. Soc.* **2007**, *129*, 9540. (f) Zeidan, R. K.; Davis, M. E. *J. Catal.* **2007**, *247*, 379. (g) Motokura, K.; Tada, M.; Iwasawa, Y. *Angew. Chem. Int. Ed.* **2008**, *47*, 9230. (h) Shylesh, S.; Wagner, A.; Seifert, A.; Ernst, S.; Thiel, W. R. *Chem. Eur. J.* **2009**, *15*, 7052. (i) Motokura, K.; Tada, M.; Iwasawa, Y. *J. Am. Chem. Soc.* **2009**, *131*, 7944. (j) Shylesh, S.; Thiel, W. R. *ChemCatChem* **2011**, *3*, 278. (k) Shang, F.; Sun, J.; Wu, S.; Liu, H.; Guan, J.; Kan, Q. *J. Colloid Interface Sci.* **2011**, *355*,

190.

[6] For Lewis acids or metal particles, and organic bases, see: (a) Waki, M.; Muratsugu, S.; Tada, M. *Chem. Commun.* **2013**, *49*, 7283. (b) Motokura, K.; Ito, Y.; Noda, H.; Miyaji, A.; Yamaguchi, S.; Baba, T. *ChemPlusChem* **2014**, *79*, 1053.

[7] For Metal complexes and organic bases, see: (a) Dickschat, A. T.; Surmiak, S.; Studer, A. *Synlett.* **2013**, *24*, 1523. (b) Dickschat, A. T.; Behrends, F.; Surmiak, S.; Weiß, M.; Eckert, H.; Studer, A. *Chem. Commun.* **2013**, *49*, 2195. (c) Liu, J.; Huo, X.; Li, T.; Yang, Z.; Xi, P.; Wang, Z.; Wang, B. *Chem. Eur. J.* **2014**, *20*, 11549.

[8] (a) Noda, H.; Motokura, K.; Miyaji, A.; Baba, T. *Angew. Chem. Int. Ed.* **2012**, *51*, 8017. (b) Noda, H.; Motokura, K.; Miyaji, A.; Baba, T. *Adv. Synth. Catal.* **2013**, *355*, 973.

[9] (a) Sakai, M.; Hayashi, H.; Miyaura, N. *Organometallics* **1997**, *16*, 4229. (b) Takaya, Y.; Ogasawara, M.; Hayashi, T.; Sakai, M.; Miyaura, N. *J. Am. Chem. Soc.* **1998**, *120*, 5579. (c) Sakuma, S.; Miyaura, N. *J. Org. Chem.* **2001**, *66*, 8944. (d) Kuriyama, M.; Tomioka, K. *Tetrahedron Lett.* **2001**, *42*, 921. (e) Reets, M. T.; Moulin, D.; Gosberg, A. *Org. Lett.* **2001**, *3*, 4083. (f) Hayashi, T.; Takahashi, M.; Takaya, Y.; Ogasawara, M. *J. Am. Chem. Soc.* **2002**, *124*, 5052. (g) Boiteau, J.-G.; Minnaard, A. J.; Feringa, B. L. *J. Org. Chem.* **2003**, *68*, 9481. (h) Otomaru, Y.; Senda, T.; Hayashi, T. *Org. Lett.* **2004**, *6*, 3357. (i) Kina, A.; Ueyama, K.; Hayashi, T. *Org. Lett.* **2005**, *7*, 5889. (j) Korenaga, T.; Osaki, K.; Maenishi, R.; Sakai, T. *Org. Lett.* **2009**, *11*, 2325. (k) Hu, X.; Zhuang, M.; Cao, Z.; Du, H. *Org. Lett.* **2009**, *11*, 4744. (l) Motokura, K.; Hashimoto, N.; Hara, T.; Mitsudome, T.; Mizugaki, T.; Jitsukawa, K.; Kaneda, K. *Green Chem.* **2011**, *13*, 2416. (m) Hara, T.; Fujita, N.; Ichikuni, N.; Wilson, K.; Lee, A. F.; Shimazu, S. *ACS Catal.* **2014**, *4*, 4040.

- [10] (a) Kina, A.; Yasuhara, Y.; Nishimura, T.; Iwamura, H.; Hayashi, T. *Chem. Asian J.* **2006**, *1*, 707. (b) Kina, A.; Iwamura, H.; Hayashi, T. *J. Am. Chem. Soc.* **2006**, *128*, 3904.
- [11] (a) Braga, A. A. C.; Morgon, N. H.; Ujaque, G.; Maseras, F. *J. Am. Chem. Soc.* **2005**, *127*, 9298. (b) Lennox, A. J. J.; Lloyd-Jones, G. C. *Angew. Chem. Int. Ed.* **2013**, *52*, 7362.
- [12] (a) Toyota, S.; Oki, M. *Bull. Chem. Soc. Jpn.* **1992**, *65*, 1832. (b) Zhu, L.; Shabbir, S. H.; Gray, M.; Lynch, V. M.; Sorey, S.; Anslyn, E. V. *J. Am. Chem. Soc.* **2006**, *128*, 1222.
- [13] For the detailed calculation method, see the Supporting Information, caption in Figure S1.
- [14] (a) Yamaguchi, K.; Yoshida, C.; Uchida, S.; Mizuno, N. *J. Am. Chem. Soc.* **2005**, *127*, 530. (b) Long, J.; Liu, G.; Cheng, T.; Yao, H.; Qian, Q.; Zhuang, J.; Gao, F.; Li, H. *J. Catal.* **2012**, *298*, 41.
- [15] (a) Adima, A.; Moreau, J. J. E.; Man, M. W. C. *J. Mater. Chem.* **1997**, *7*, 2331. (b) Bied, C.; Gauthier, D.; Moreau, J. J. E.; Man, M. W. C. *J. Sol-Gel Sci. Technol.* **2001**, *20*, 313.
- [16] (a) Schwartz, J. *Acc. Chem. Res.* **1985**, *18*, 302. (b) Fierro, J. L. G.; Merchán, M. D.; Rojas, S.; Terreros, P. *J. Mol. Catal. A: Chem.* **2001**, *166*, 255.
- [17] (a) DeBeer, S.; Kiser, C. N.; Mines, G. A.; Richards, J. H.; Gray, H. B.; Solomon, E. I.; Hedma, B.; Hodgson, K. O. *Inorg. Chem.* **1999**, *38*, 433. (b) Battiston, A. A.; Bitter, J. H.; Koningsberger, D. C. *J. Catal.* **2003**, *218*, 163.
- [18] When a complex possessing a nitrogen ligand was used for the reference compound on fitting analysis for SiO₂/diamine/Rh/NET₂-a, similar result was obtained.

[19] Sezgin, A.; Akbey, Ü.; Graf, R.; Bozkurt, A.; Baykal, A. *J. Polym. Sci. Part B: Polym. Phys.* **2009**, *47*, 1267.

[20] The boronic acid was generated by the hydrolysis of the aryl–Rh species, and was confirmed by liquid state ^{11}B NMR of the filtrate after washing the sample with D_2O .

Table 1: Elemental analyses of silica-supported Rh catalysts.

Catalyst	Molar ratio of raw materials (Rh(=diamine)/tertiary amine) ^[a]	C (mmol /g) ^[b]	N (mmol /g) ^[b]	Rh (mmol /g) ^[b]	Amount of tertiary amine (mmol/g) ^[c]
SiO ₂ /diamine/Rh-a	-	6.38	1.07	0.528	-
SiO ₂ /diamine/Rh-b	-	2.14	0.15	0.074	-
SiO ₂ /diamine/Rh/NEt ₂ -a	1/1	8.21	1.31	0.412	0.44
SiO ₂ /diamine/Rh/NEt ₂ -b	1/1	2.63	0.21	0.054	0.07
SiO ₂ /diamine/Rh/NEt ₂ -c	1/7	4.51	0.59	0.064	0.46
SiO ₂ /diamine/Rh/NEt ₂ -d	1/15	7.33	1.04	0.065	0.91
SiO ₂ /diamine/Rh/NEt ₂ -e	1/1	7.16	1.15	0.319	0.38
SiO ₂ /diamine/Rh/NEt ₂ -f	1/1	4.99	0.80	0.227	0.27
SiO ₂ /diamine/Rh/NEt ₂ -g	1/1	3.64	0.42	0.109	0.14
SiO ₂ /diamine/Rh/Me	-	5.93	0.83	0.365	-
SiO ₂ /NEt ₂	-	6.46	0.83	-	0.83

[a] Charged molar ratio of the diamine/tertiary amine. Details of the amounts of raw materials are summarized in Table S1, Supporting Information.

[b] Amount of C and N contents were determined by elemental analysis. Amount of the Rh was determined by inductively coupled plasma–atomic emission spectroscopy (ICP-AES).

[c] Tertiary amine content was calculated as follows: (Amount of tertiary amine) = (total amount of nitrogen) – (Amount of Rh) × 2

Table 2. Curve-fitting analysis for the prepared silica-supported catalysts.^[a]

Sample	$N^{[b]}$	r (Å) ^[c]	σ^2 (Å ² × 10 ⁻³) ^[d]	ΔE_0 (eV)	R_f (%)
SiO ₂ /diamine/Rh/NEt ₂ -a	6.8 ± 1.5	2.10 ± 0.02	5.44 ± 1.75	-8.46 ± 3.81	0.022
SiO ₂ /diamine/Rh/NEt ₂ -a ^[e]	6.6 ± 1.4	2.10 ± 0.02	5.65 ± 1.71	-9.09 ± 3.74	0.022
SiO ₂ /diamine/Rh/NEt ₂ -b	6.6 ± 1.0	2.10 ± 0.01	5.57 ± 1.27	-7.01 ± 2.58	0.018
SiO ₂ /diamine/Rh/NEt ₂ -f	6.9 ± 1.4	2.07 ± 0.01	5.43 ± 1.71	-7.21 ± 3.37	0.010
SiO ₂ /diamine/Rh-a	6.8 ± 1.5	2.09 ± 0.02	5.35 ± 1.68	-10.2 ± 4.06	0.022
SiO ₂ /diamine/Rh/Me	6.8 ± 1.3	2.10 ± 0.01	5.41 ± 1.62	-7.80 ± 3.30	0.017

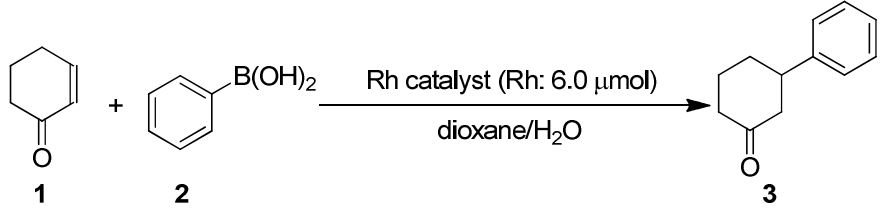
[a] Fitting range of the R -space was 1.2–2.0 (Å). The k range for Fourier transformation was $k = 3$ –13 (Å⁻¹).

[b] Coordination number.

[c] Bond distance.

[d] Debye –Waller factor.

[e] Recovered SiO₂/diamine/Rh/NEt₂-a.

Table 3. 1,4-Addition between cyclohexenone and phenylboronic acid using Rh catalysts.^[a]


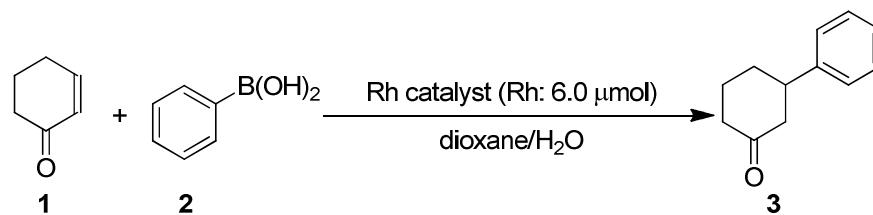
Entry	Catalyst	Conversion of 1 (%) ^[b]	Yield of 3 (%) ^[b]
1	SiO ₂ /diamine/Rh/NEt ₂ -a	28	28
2	SiO ₂ /diamine/Rh-a	10	10
3	SiO ₂ /diamine/NEt ₂ ^[c]	0	0
4	None	0	0
5	SiO ₂ /diamine/Rh-a + free tertiary amine ^[d]	8	8
6	SiO ₂ /diamine/Rh/NEt ₂ -a + free tertiary amine ^[d]	11	11
7	SiO ₂ /diamine/Rh-a + SiO ₂ /NEt ₂	10	10
8	SiO ₂ /diamine/Rh/Me	7	7

[a] Reaction conditions: cyclohexenone (**1**) (1.0 mmol), phenyl boronic acid (**2**) (1.5 mmol), Silica-supported Rh catalyst (Rh: 6.0 μmol), 1,4-dioxane/H₂O (10/1, 2.0 mL), 60 °C, 1 h.

[b] Determined by ¹H NMR using internal standard technique. 1,3,5-Triisopropylbenzene was used as an internal standard.

[c] 1.3 × 10⁻² g SiO₂/diamine/NEt₂ was used.

[d] diethylbutylamine (6.0 μmol) was added.

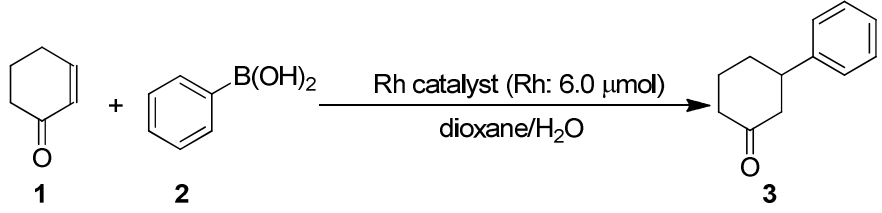
Table 4. Effect of the amount of immobilized tertiary amine on the product yield.^[a]

Catalyst	Rh (mmol/g)	Tertiary amine (mmol/g)	Yield of 3 (%) ^[b]
SiO ₂ /diamine/Rh-b	0.074	-	4
SiO ₂ /diamine/Rh/NEt ₂ -b	0.054	0.07	6
SiO ₂ /diamine/Rh/NEt ₂ -c	0.064	0.46	12
SiO ₂ /diamine/Rh/NEt ₂ -d	0.065	0.91	30

[a] Reaction conditions: cyclohexenone (**1**) (1.0 mmol), phenylboronic acid (**2**) (1.5 mmol), Silica-supported Rh catalyst (Rh: 6.0 μmol), 1,4-dioxane/H₂O (10/1, 2.0 mL), 60 °C, 1 h.

[b] Determined by ¹H NMR using internal standard technique. 1,3,5-Triisopropylbenzene was used as an internal standard.

Table 5. Effect of the total amount of immobilized Rh complex and tertiary amine on the product yield.^[a]

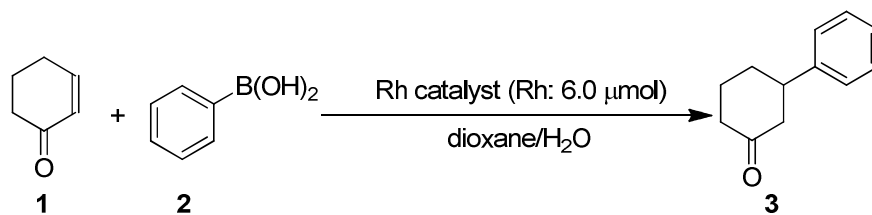


The reaction scheme shows cyclohexenone (1) reacting with phenylboronic acid (2) in the presence of a Rh catalyst (Rh: 6.0 μmol) in a dioxane/H₂O solvent system to produce 1-phenylcyclohexanone (3).

Catalyst	Rh (mmol/g)	Tertiary amine (mmol/g)	Total amount of organic functionalities (mmol/g)	Yield of 3 (%) ^[b]
SiO ₂ /diamine/Rh/NEt ₂ -a	0.412	0.44	0.85	28
SiO ₂ /diamine/Rh/NEt ₂ -e	0.319	0.38	0.70	16
SiO ₂ /diamine/Rh/NEt ₂ -f	0.227	0.27	0.50	13
SiO ₂ /diamine/Rh/NEt ₂ -g	0.109	0.14	0.25	7
SiO ₂ /diamine/Rh/NEt ₂ -b	0.054	0.07	0.12	6

[a] Reaction conditions: cyclohexenone (**1**) (1.0 mmol), phenylboronic acid (**2**) (1.5 mmol), SiO₂/diamine/Rh/NEt₂ (Rh: 6.0 μmol), 1,4-dioxane/H₂O (10/1, 2.0 mL), 60 °C, 1 h.

[b] Determined by ¹H NMR using internal standard technique. 1,3,5-Triisopropylbenzene was used as an internal standard.

Table 6. Effect of the total amount of immobilized organic functionalities on the product yield.^[a]

Catalyst	Rh (mmol/g)	Tertiary amine (mmol/g)	Total amount of organic functionalities (mmol/g)	Yield of 3 (%) ^[b]
SiO ₂ /diamine/Rh/NEt ₂ -a	0.412	0.44	0.85	28
SiO ₂ /diamine/Rh/NEt ₂ -d	0.065	0.91	0.98	30
SiO ₂ /diamine/Rh/NEt ₂ -c	0.064	0.46	0.52	12
SiO ₂ /diamine/Rh/NEt ₂ -f	0.227	0.27	0.49	13

[a] Reaction conditions: cyclohexenone (**1**) (1.0 mmol), phenylboronic acid (**2**) (1.5 mmol), SiO₂/diamine/Rh/NEt₂ (Rh: 6.0 μmol), 1,4-dioxane/H₂O (10/1, 2.0 mL), 60 °C, 1 h.

[b] Determined by ¹H NMR using internal standard technique. 1,3,5-Triisopropylbenzene was used as an internal standard.

Table 7. 1,4-Addition using various phenylboronic acids with cyclohexenone catalyzed by SiO₂/diamine/Rh/NEt₂-a.^[a]

Entry	Phenylboronic acid	Product	Yield (%) ^[b]
1 ^[c]			>99
2			85
3			97
4			80 ^[d]
5			84
6			51 (42) ^[e]
7			86 (70) ^[e]

[a] Reaction conditions: cyclohexenone (**1**) (0.5 mmol), phenylboronic acid (0.75 mmol), SiO₂/diamine/Rh/NEt₂-a (Rh: 6.0 μmol), 1,4-dioxane/H₂O (10/1, 0.5 mL), 80 °C, 1 h.

[b] Determined by ¹H NMR using internal standard technique. 1,3,5-Triisopropylbenzene was used as an internal standard.

[c] Reaction conditions: cyclohexenone (**1**) (0.5 mmol), phenylboronic acid (0.75 mmol), SiO₂/diamine/Rh/NEt₂ (Rh: 12.0 μmol), 1,4-dioxane/H₂O (10/1, 0.5 mL), 60 °C, 1 h.

[d] 24 h.

[e] SiO₂/diamine/Rh-a was used as a catalyst.

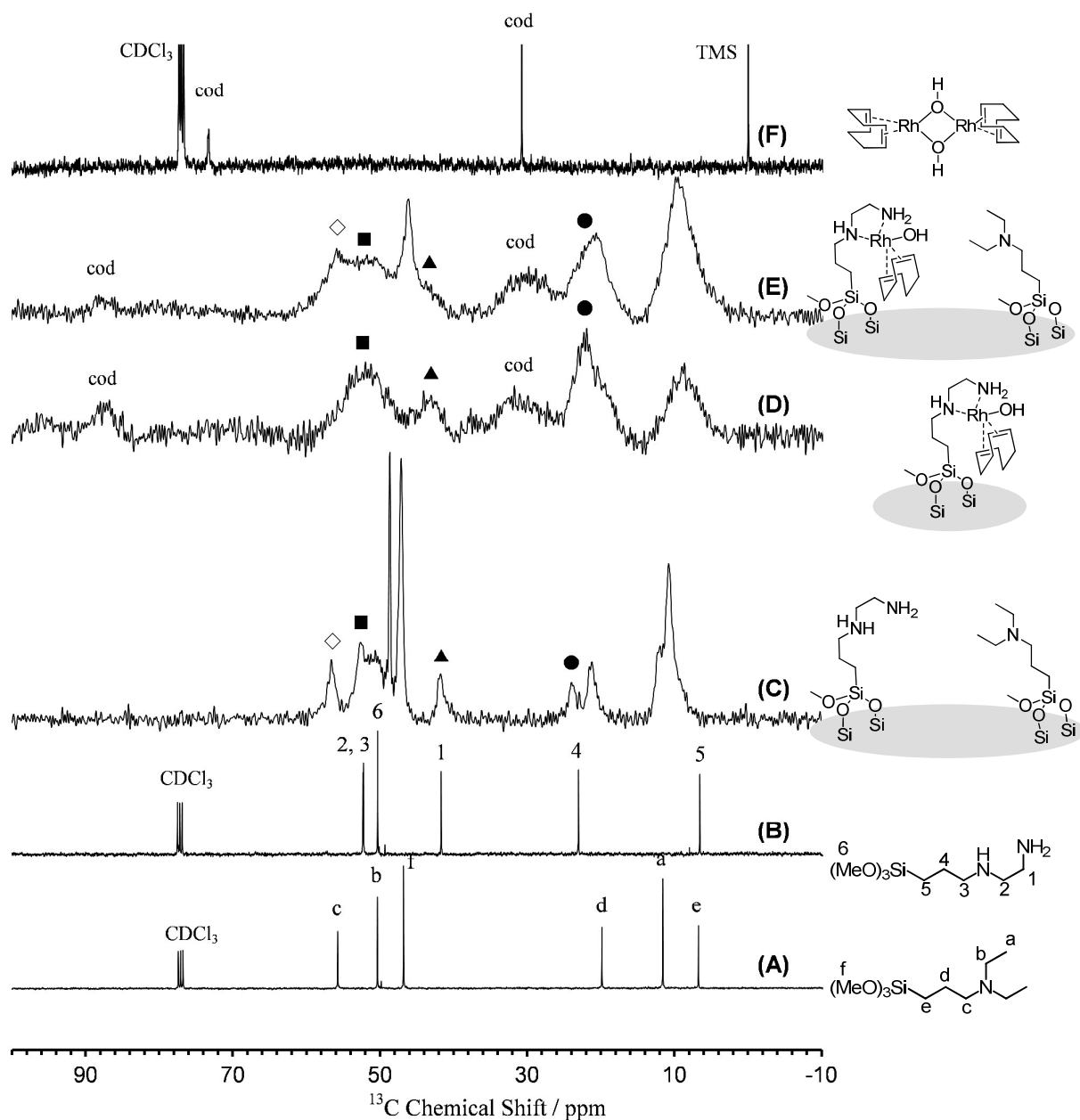


Figure 1. Liquid-state ^{13}C NMR spectra of (A) 3-diethylaminopropyltrimethoxysilane, and (B) 3-(2-aminoethylamino)propyltrimethoxysilane. Solid-state ^{13}C CP/MAS NMR spectra of (C) $\text{SiO}_2/\text{diamine}/\text{NEt}_2$, (D) $\text{SiO}_2/\text{diamine}/\text{Rh-a}$, and (E) $\text{SiO}_2/\text{diamine}/\text{Rh}/\text{NEt}_2\text{-a}$. (F) Liquid-state ^{13}C NMR spectrum of $[\text{Rh}(\text{cod})\text{OH}]_2$.

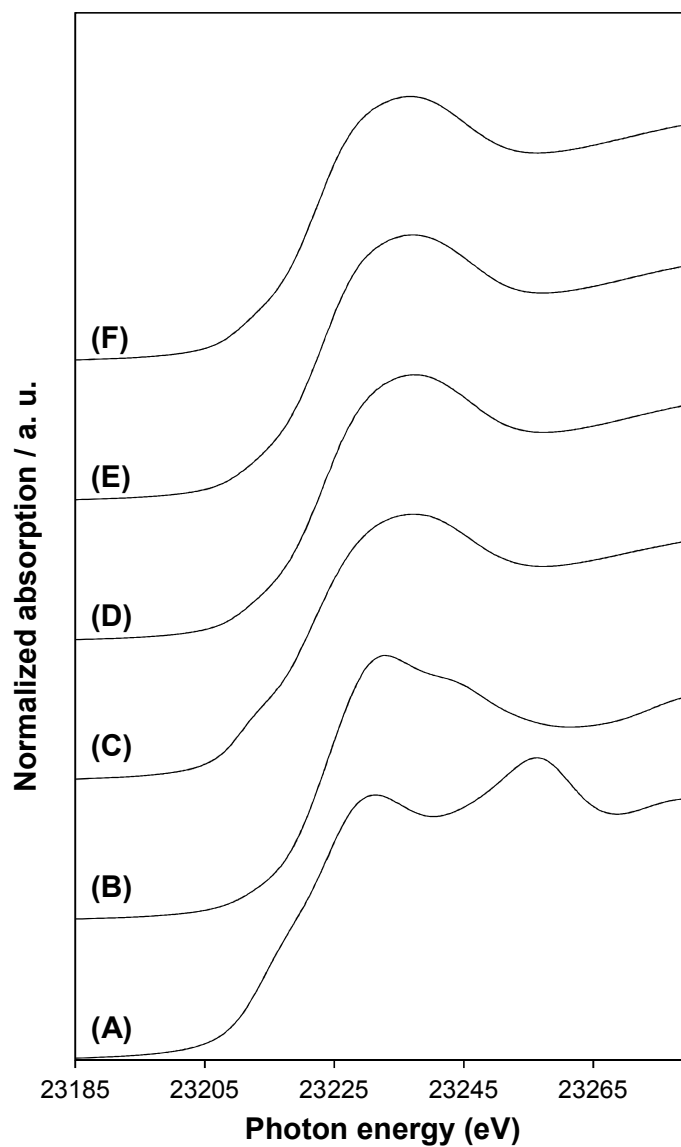


Figure 2. Rh K-edge XANES spectra of (A) Rh foil, (B) Rh_2O_3 , (C) $[\text{Rh}(\text{cod})\text{OH}]_2$, (D) $\text{SiO}_2/\text{diamine}/\text{Rh}/\text{NET}_2\text{-a}$, (E) $\text{SiO}_2/\text{diamine}/\text{Rh-a}$, and (F) recovered $\text{SiO}_2/\text{diamine}/\text{Rh}/\text{NET}_2\text{-a}$ after the 1,4-addition between **1** and **2**.

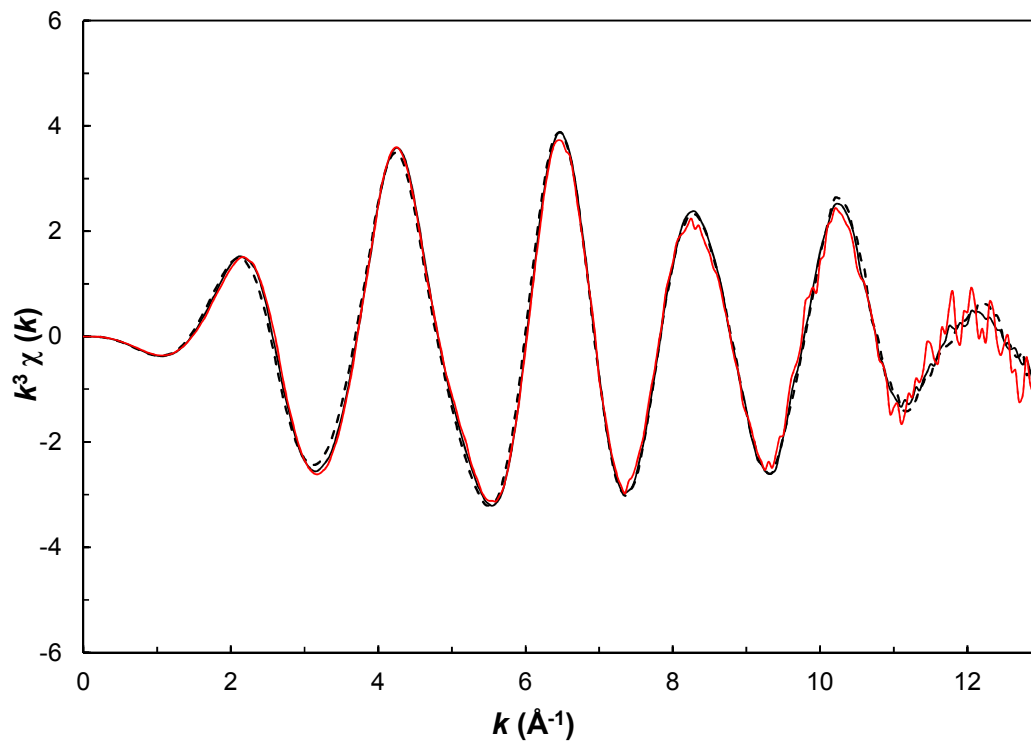


Figure 3. EXAFS spectra of SiO₂/diamine/Rh/NEt₂-a (black solid line), SiO₂/diamine/Rh-a (black dashed line), and SiO₂/diamine/Rh/NEt₂-b (red solid line).

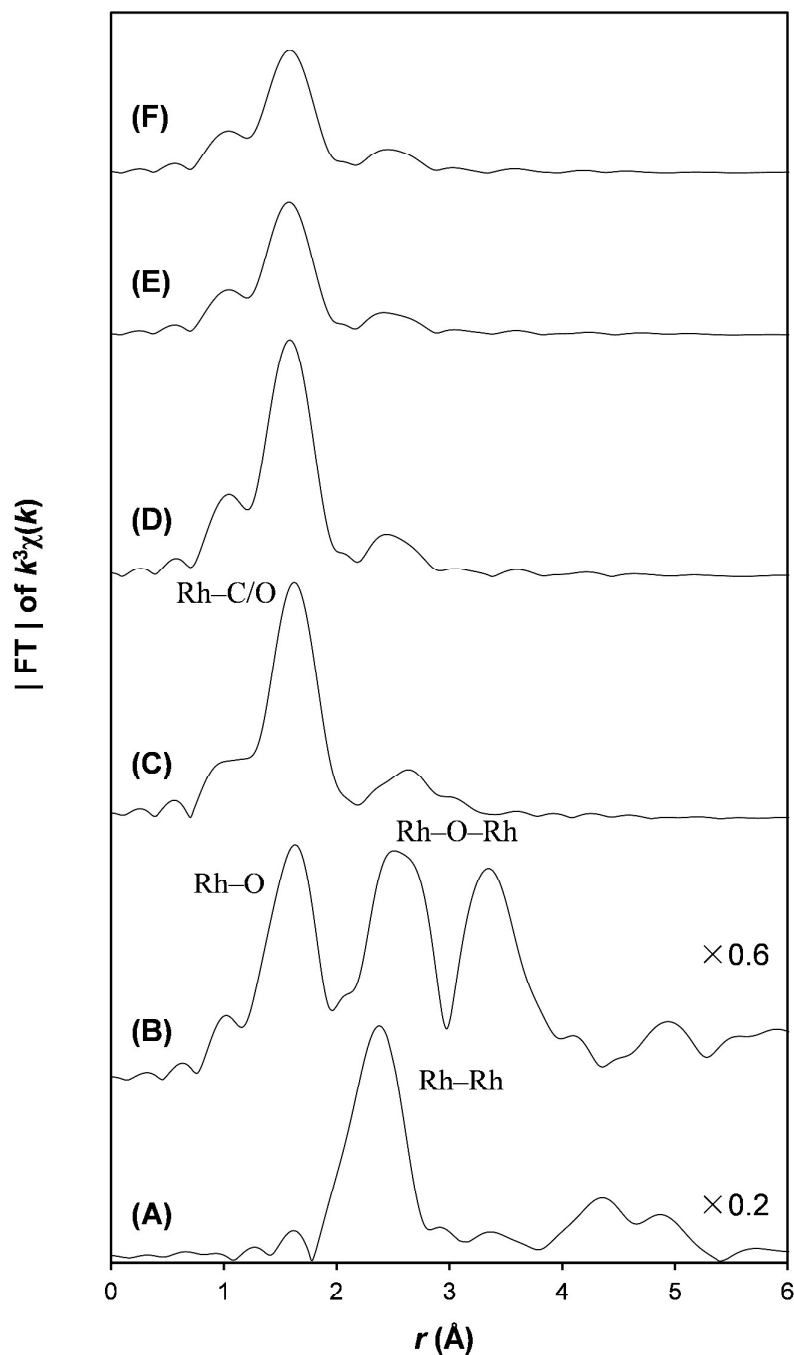


Figure 4. Fourier transforms of the k^3 -weighted Rh K-edge EXAFS spectra for (A) Rh foil, (B) Rh_2O_3 , (C) $[\text{Rh}(\text{cod})\text{OH}]_2$, (D) $\text{SiO}_2/\text{diamine}/\text{Rh}/\text{NET}_2\text{-a}$, (E) $\text{SiO}_2/\text{diamine}/\text{Rh-a}$, and (F) recovered $\text{SiO}_2/\text{diamine}/\text{Rh}/\text{NET}_2\text{-a}$ after the 1,4-addition between 1 and 2. The k range for FT was $k = 3\text{--}13$ (\AA^{-1}).

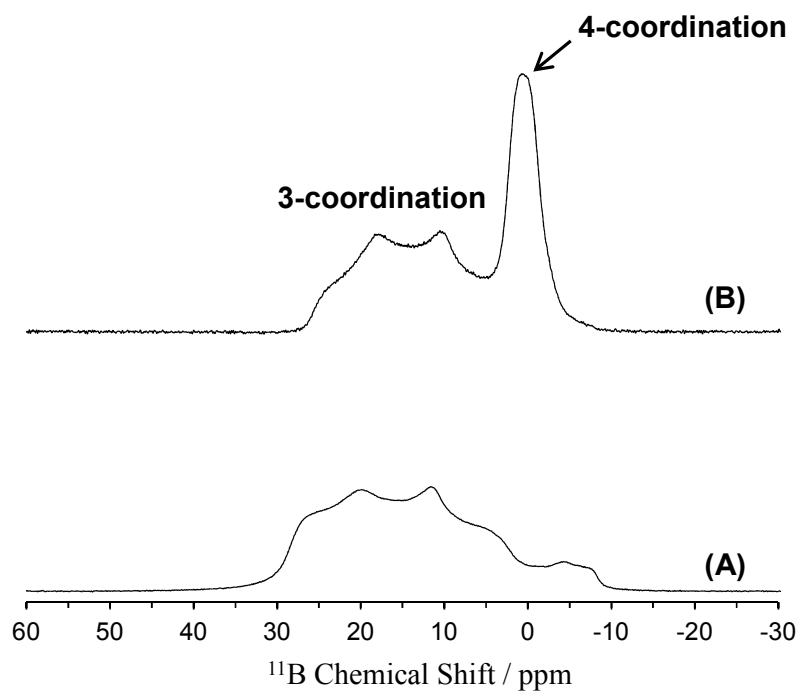


Figure 5. Solid-state ^{11}B MAS NMR spectra of (A) phenylboronic acid and (B) phenylboronic acid with $\text{SiO}_2/\text{NEt}_2$.

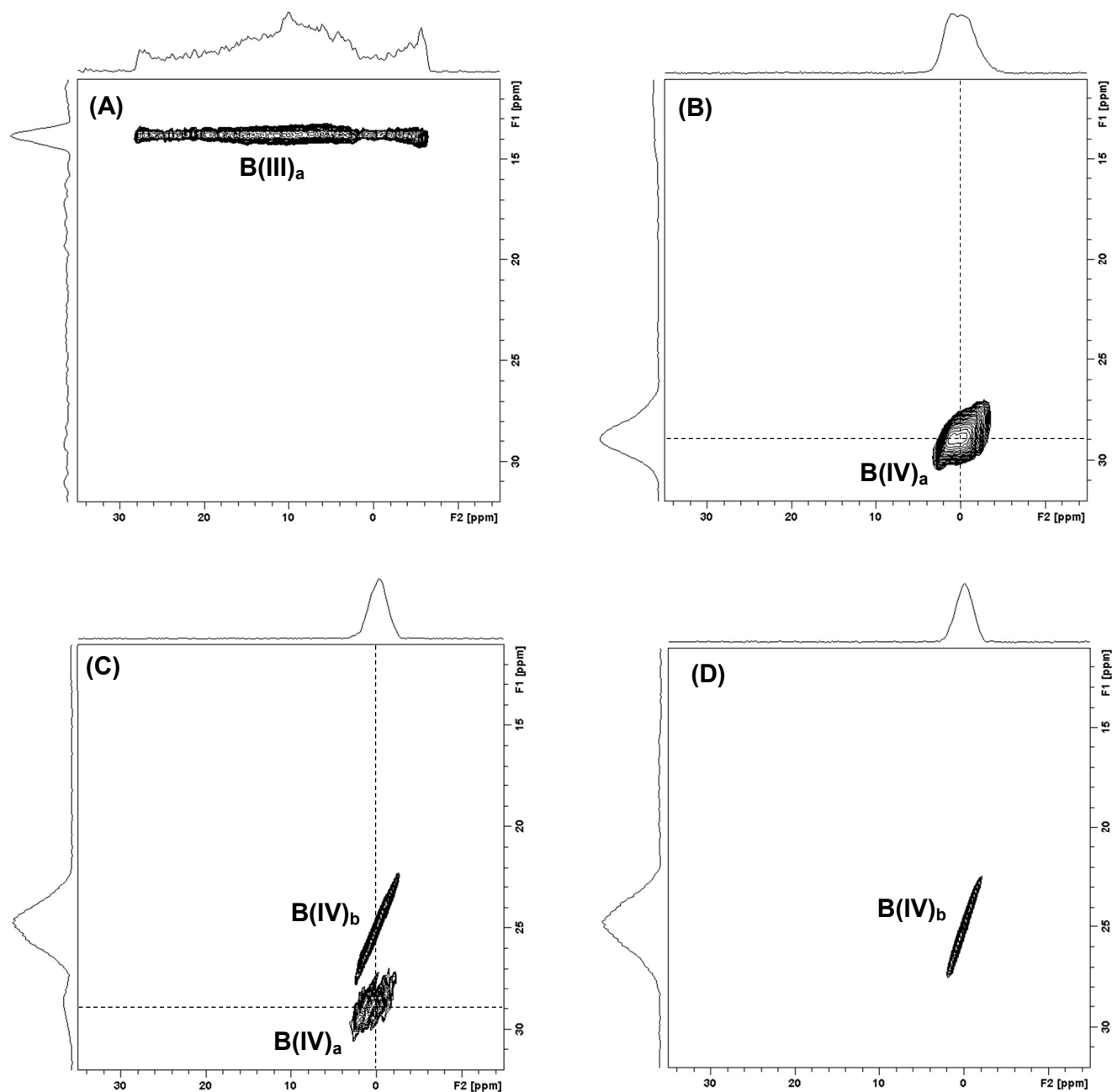


Figure 6. Solid-state ^{11}B MQ MAS NMR spectra of (A) phenylboronic acid, (B) phenylboronic acid with $\text{SiO}_2/\text{NET}_2$, (C) phenylboronic acid with $\text{SiO}_2/\text{diamine}/\text{Rh}/\text{NET}_2$ (**4**), and (D) After treatment of **4** with cyclohexenone.

TOC graphic

